RSC Advances

PAPER

View Article Online
View Journal | View Issue

Cite this: *RSC Adv.*, 2023, **13**, 16724

Emilia sonchifolia leaf extract-mediated green synthesis, characterization, *in vitro* biological activities, photocatalytic degradation and *in vivo Danio rerio* embryo toxicity of copper nanoparticles

Vainath Praveen Sankara Narayanan, Sabeena Gabrial Kathirason, Pushpalakshmi Elango, Rajaduraipandian Subramanian, Sivagurusundar. R and Annadurai Gurusamy *

The green-mediated synthesis of copper nanoparticles is of great interest in nanotechnology and is regarded as a low-cost and environmentally beneficial method. Herein, *Emilia sonchifolia* leaf extract was employed as a reducing and capping agent for the green production of copper nanoparticles. In this work, we focused on the *in vivo* and *in vitro* biological studies of copper nanoparticles, which were evaluated in zebrafish (*Danio rerio*) embryos. The biological effects from the *in vitro* studies of the copper nanoparticles included cytotoxicity (in human cells) and anti-diabetic, anti-inflammatory, and antibacterial activity. Furthermore, the effectiveness of the greenly produced copper nanoparticles for photocatalysis was also evaluated, and then SEM-EDX, FTIR, XRD, TGA and UV-vis spectroscopy were used to characterise the copper nanoparticles. The results of the toxicity test on zebrafish embryos demonstrated that the green-produced copper nanoparticles had a significantly low harmful effect. According to the results, the copper nanoparticles showed dose-dependent cytotoxicity against human keratinocytes (HaCaT) and human breast cancer cells (MCF-7), which was higher than that of the *Emilia sonchifolia* leaf extract. The green copper nanoparticles also demonstrated more potent anti-inflammatory, antibacterial and anti-diabetic properties. In the photocatalytic experiment, the produced copper nanoparticles successfully degraded the organic methylene blue dye. Thus, it can be concluded that copper nanoparticles can be employed for drug administration in both *in vitro* and *in vivo* settings in biomedical applications. Additionally, as catalysts, these copper nanoparticles can be employed for the removal of organic dyes.

Received 21st January 2023
Accepted 10th February 2023

DOI: 10.1039/d3ra00454f

rsc.li/rsc-advances

1. Introduction

Nanoparticles have attracted significant attention in diverse fields due to their remarkable properties compared to their bulk counterparts.[1,2] Because nanoparticles are tiny units with a size in the range of 1 to 100 nm, they have unique attributes including shape, dispersion, and morphology.[1,3]

Green-mediated synthesis is considered to be the best technique among different synthesis strategies due to the reduction in the use of reagents, photochemical and electrochemical reactions, heat, *etc.*[4] Accordingly, the green synthesis of nanoparticles utilizing plant extracts offers an alternative to overcome many problems associated with their synthesis, which is a simple, environmentally friendly and efficient technique. The extracts of plants are very cheap and stable against harsh reaction conditions.[5] Nevertheless, the green method is limited by the extraction of green materials, long reaction times, and poor product quality. For instance, the synthesis period is lengthy, and the raw components are not easily accessible. Recently, the potential weaknesses and limitations of green methods were reviewed.[99]

Numerous works investigated the use of plant extracts, for example, *Solanum lycopersicum*,[6] *Eclipta prostrata*,[3] *Punica granatum*,[7] *Plantago asiatica*,[8] *Gnidia glauca* and *Plumbago zeylan*ica,[9] *Uncaria gambir Roxb*,[10] *Camellia sinen*sis,[11] *Moringa oleifera*,[12] *Crataegus pontica* L,[13] dates,[14] tea leaves,[15] *Murraya Koenigii* leaves,[16] tomato leaves,[6] *Aegle marme*los leaves,[17] for the synthesis of copper nanoparticles. Consequently, different plants produce diverse nanoparticle attributes.

Despite the fact that it is rarely used, *Emilia sonchifolia* is recorded in Ayurveda and Siddha medicine. Ayurveda suggests that this plant can be employed for the treatment of

Sri Paramakalyani Centre of Excellence in Environmental Sciences, Manonmaniam Sundaranar University, Alwarkurichi-627412, India. E-mail: gannadurai@msuniv.ac.in; annananoteam@gmail.com

gastropathy, loose bowels, ophthalmia, nyctalopia, cuts and wounds, irregular fevers, pharyngodynia and asthma.[18] In Siddha medicine, this plant is suggested for the treatment of intestinal worms and bleeding piles.[19] The *Emilia sonchifolia* plant is reported in ethnomedicine to have therapeutic advantages in treating diarrhoea, night blindness, sore throat, rashes, measles, motion sickness, eye and ear afflictions, fever, stomach tumors, jungle fever, asthma, liver illnesses, eye irritation, ear infection and chest pain.[20] In China, *Emilia sonchifolia* leaves are utilized for the treatment of looseness of the bowels, roundworm infestations, wounds and abscesses, the flu, burns and snake bites.[20] In India, the administration of the leaf glue one spoonful daily before bed for around 2–3 months is prescribed to treat night visual impairment.[21] The crushed leaves are scoured on the brow to soothe cerebral pain.[22–24] *Emilia sonchifolia* leaf extract is a fantastic source of antidiabetic and anti-inflammatory activity and cytotoxicity and a novel way to make nanoparticles safer and more stable, where the synthesis of stable nanoparticles using *Emilia sonchifolia* leaf extract is a quick, easy and safe procedure.[25]

Copper nanoparticles are widely applied in industry, medicine, equipment, *etc.* Because of their desirable properties such as high electrical conductivity, low electrochemical migration behavior, high melting point and low cost.[27,28] In the literature, reports[26] show that copper nanoparticles can be utilized as alternatives to metals in various applications, for example, in inkjet printing, heat transfer, gas-phase catalysis, photocatalysis and electrocatalysis.[27] Furthermore, the green-mediated synthesis of copper nanoparticles has been reported using bottom-up techniques. Considering the biomedical applications of copper nanoparticles, the solvent, stabilizing agent and reducing agent used for their green-mediated synthesis need to be non-toxic. Recently, green-synthesized nanoparticles have received significant attention due to their photocatalytic ability to degrade organic dyes.[28]

In vivo studies can provide an accurate assessment of the safety, toxicity, and efficacy of a complicated model. Furthermore, breakthroughs have been achieved in the replication of human diseases in animals with excellent accuracy.[98] The zebrafish embryo toxicity test is employed as a conventional *in vivo* approach to assess evolving toxicity. Thus, recently, zebrafish have been employed as different and effective *in vivo* models to evaluate the biosafety of various nanoparticles.[98] Zebrafish embryos develop significantly faster than mammalian models, thereby decreasing the time required to perform experiments. In preclinical studies, the zebrafish (*Danio rerio*) has emerged as a crucial platform for drug delivery and toxicity screening. Zebrafish are not only used for toxicity testing, but researchers are also developing transgenic Zebrafish models through genetic modification and focusing on their transformation for diseases such as digestive system disorders, cardiovascular and neurological diseases, diabetes, malignant growths, and inflammation.[29] Copper nanoparticles may be effective agents in a variety of environmental and biological applications, which will be investigated in the near future.

Consequently, herein, we report for the first time, the use of leaf extracts from the medicinal plant *Emilia sonchifolia* to synthesise copper nanoparticles. This unique green synthesis is pollutant free and eco-friendly. Ultraviolet-visible spectroscopy, Fourier transform infrared spectroscopy, X-ray diffraction, thermogravimetric analysis and scanning electron microscopy-energy dispersive X-ray were used to characterise the green copper nanoparticles. The aim of this work was to determine the *in vitro* anti-diabetic, anti-inflammatory, and cytotoxicity activity of the green-produced copper nanoparticles employing *Emilia sonchifolia* leaf extract as a reducing agent and their photocatalytic efficacy for the degradation of organic dyes. Zebrafish embryos were used as a model animal for the toxicity analysis.

2. Experimental

2.1 Plant collection

Emilia sonchifolia, a traditional and medicinally essential plant, was obtained from Western Ghats in Tamil Nadu.

2.2 Materials

Copper nitrate utilised in this investigation was of analytical quality and bought from Sigma Aldrich. Filtration was accomplished using Whatman No. 1 filter sheets. Distilled water was used twice. Before embarking on the experiment, all glassware was thoroughly sanitized, rinsed with double distilled water, and dried in a hot air oven.

2.3 Preparation of *Emilia sonchifolia* leaf extract

As shown in Fig. 1, *Emilia sonchifolia* leaves were collected and rinsed thoroughly in double distilled water, and then chopped into tiny pieces. Subsequently, 15 g of leaves was weighed and placed in a 250 mL beaker with 150 mL of water. After around 20 min, the extract was filtered through Whatman No. 1 filter paper. The extract supernatant was collected and kept at 40 °C for future use.

2.4 Green-mediated synthesis of copper nanoparticles

Under continuous stirring, a 30 mL solution of *Emilia sonchifolia* leaf extract was dropped into 100 mL of 1 mM copper nitrate solution. The solution was heated at 70 °C for 20 min on a magnetic stirrer. After the addition of all the leaf extract, the mixture was incubated for 24 h. Within a short period, the

Fig. 1 Preparation of *Emilia sonchifolia* leaf extract, which was employed as a reducing agent for the synthesis of copper nanoparticles.

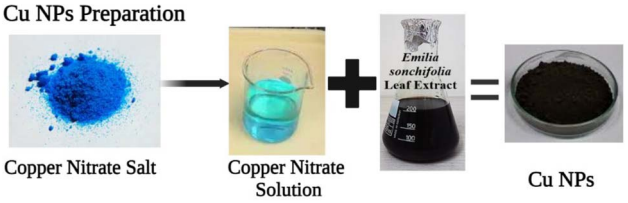

Fig. 2 Green-mediated synthesis of copper nanoparticles.

brownish-green solution changed to brownish black, indicating the creation of copper nanoparticles (Fig. 2). The majority of the novel secondary metabolites found in *Emilia sonchifolia* extracts, including phenolic acid, flavonoids, alkaloids, and terpenoids, are responsible for reducing ionic Cu into zero valent Cu, and finally the formation of copper nanoparticles, together with an increase in the thermodynamic stability of the copper nanoparticles.[100] Subsequently, the solution was refrigerated at 4 °C. Finally, the precipitate settled at the bottom of the conical flask. The solution was centrifuged for 15 min at 10 000 rpm and dispersed in double-distilled water before being washed in ethanol to eliminate any biological contaminants.[30]

2.5 Antibacterial activity

The qualitative well diffusion approach was used to assess the antibacterial activity of the copper nanoparticles.[31] The bactericidal effect of copper nanoparticles has been linked to their tight interaction with the bacterial membranes. The copper nanoparticles were tested for antibacterial activity against a variety of pathogenic bacteria, including *E. coli*, *Staphylococcus aureus*, *Pseudomonas*, *Enterobacter*, and *Bacillus*. Nutrient agar was employed to culture the bacteria. Mueller–Hinton agar (MHA) plates were inoculated with each microbe. The wells were set on the hardened medium once it had solidified. In each plate, test wells (5 mm) were created, and the synthesized copper nanoparticles were gently added to the wells at different concentrations ranging from 25 μL to 100 μL. The Petri dishes were maintained at 37 °C for 24 h before measuring the widths of the inhibitory zones around the samples in millimetres. The results for these plates for each sample were averaged, and this value was used to calculate the minimum inhibitory concentration (MIC) of the copper nanoparticles against each microbe.[32]

2.6 Zebrafish and embryo maintenance

Each test was performed in accordance with the (OECD) Organization for Economic Cooperation and Development proper creature practise standards and policies.[33] Wild-type zebrafish were maintained, and zebrafish were purchased from a nearby aquarium fish dealer. Fish breeding was facilitated by maintaining a 3 : 1 ratio of females to males. They were maintained for 10 h in the dark and 14 h in light as part of the photoperiodism. After breeding, the water temperature was maintained at 26 °C ± 2 °C using a suitable staple and *Artemia*. In addition to being reared in E_3 medium (5 mM L^{-1} sodium chloride, 0.18 mM L^{-1} potassium chloride, 0.33 mM L^{-1} calcium chloride, and 0.33 mM L^{-1} magnesium sulphate), the embryos were maintained at 28.5 °C and came from spontaneous spawning.[34]

2.7 Toxicity study of green-mediated synthesized copper nanoparticles in embryo zebrafish

In vivo hazardous quality evaluation of the copper nanoparticles was attempted using *Emilia sonchifolia* leaf extract, and a life model was created. Briefly, *Emilia sonchifolia* leaf extract was used to facilitate the synthesis of copper nanoparticles, and their effect on 30 underdeveloped zebrafish 24 hpf for a period of 72 h. The concentrations used ranged from 450 mg L^{-1} to 500 mg L^{-1} in the E_3 mode. The arrangement was hatched at 28 ± 1 °C and had a photoperiod of 10 h in the dark and 14 h in the light. At each break, perception by microscopy was carried out to visualise the evolving and morphological variants. The birth survey was reliable because fewer incubated underdeveloped organisms were present by 72 hpf than in the natural collection. Compared to the control group, a few incipient organisms were terminated after 72 hpf, indicating a death rate. The exploratory tests were conducted in groups of three for each test.[34] The number of hatched larvae, dead embryos, and embryos with developmental abnormalities was tallied. Under a binocular microscope, the growth stages of the eggs were observed. We considered pericardial edema, scoliosis, and a reduction in body size as abnormalities in the zebra fish embryos. At the conclusion of the experiment, the population mortality index, proportion of morphologically aberrant zebrafish embryos, hatching rate, and morphological variance among survivors were calculated.[35]

2.8 Anti-diabetic activity

2.8.1 α-Glucosidase inhibitory activity. The produced copper nanoparticles were combined with α-glucosidase (0.05 g α-glucosidase in 50 mL ice-cold distilled water), and then sonicated for 20 min at room temperature.[36] *P*-Nitrophenyl-D-glucopyranoside (4 mM) was added to the mixture as a substrate in potassium phosphate buffer to initiate the reaction. After 10 min of incubation at 37 °C, the process was stopped by adding sodium carbonate in a certain ratio (2 mL, 0.2 M). As a control, a tube containing α-glucosidase with 100% enzyme activity and no nanomaterials was used. The release of *p*-nitrophenyl-D-glucopyranoside as a percentage of inhibition was calculated to measure the α-glucosidase inhibitory activity using the formula below.

$$I_{\alpha\text{-glucose}}\,(\%) = A_{405\ \text{control}} - A_{405\ \text{sample}}/A_{405\ \text{control}} \times 100$$

2.9 Anti-inflammatory activity

2.9.1 Protein denaturation-egg albumin. A reaction mixture (5 mL) of 0.4 mL of fresh hen egg albumin, 5.6 mL of phosphate-buffered saline (pH 5.4), and 4 mL of different concentrations of copper nanoparticles (10–80 μL mL^{-1}) was incubated at 35 °C for 25 min, and then heated at 40 °C for 5 min in a biochemical oxygen demand incubator. An

equivalent volume of pure water served as the control. After cooling, the absorbance was measured at 660 nm using the vehicle as a blank. A standard solution with various concentrations was used and treated similarly for absorbance.[37,38] The following equation was used to calculate the percentage of protein denaturation inhibition:

$$\%\ \text{Inhibition} = 100 \times \frac{V_t}{V_c - 1}$$

where V_t represents the absorbance of the test sample and V_c represents the absorbance of the control. The percentage inhibition with respect to the standard was plotted against the treatment sample concentration.

2.10 Cytotoxicity activity

2.10.1 3-(4,5-Dimethylthiazol-2-yl)-2,5-diphenyltetrazolium bromide reduction assay. Using the traditional 3-(4,5-dimethylthiazol-2-yl)-2,5-diphenyltetrazolium bromide reduction assay, a cell viability study was carried out to determine the cytotoxic and anticancer effects of the *Emilia sonchifolia*, green-mediated copper nanoparticles.[39–41] Briefly, human keratinocyte (HaCaT) and human breast cancer (MCF-7) cells were seeded in 96-well plates at a density of 4000 cells per well. The cells were cultured for 24 h in an incubator containing 2% carbon dioxide at 35 °C. Following a 24 h seeding period, the medium inside the wells was changed and different concentrations of *Emilia sonchifolia*, green-mediated copper nanoparticles (10–120 μL mL^{-1}) were added. Then, the wells were incubated for a further 24–72 h at 37 °C. The old medium was replaced with 200 mL of new medium, 10 mL of 3-(4,5-dimethylthiazol-2-yl)-2,5-diphenyltetrazolium solution was added to each well, and the plates were incubated for an additional 3 h to determine the cell viability. Subsequently, the 3-(4,5-dimethylthiazol-2-yl)-2,5-diphenyltetrazolium solution was removed, and 200 μL of dimethyl sulfoxide was applied to each well and incubated overnight for 50 min in the dark. Finally, the solution was diluted and its absorbance was read at 492 nm using a microplate reader.

2.11 Photocatalytic activity

The performance of the copper nanoparticles for the removal of methylene blue dye (MB) in an aqueous solution was assessed. To guarantee the process of dye removal, 0.01 g of copper nanoparticles and 1 mL of methylene blue dye solution containing 10 ppm were mixed in a 10 mL vial and stirred at room temperature for 25 min.[42,43] The sample was removed from the vial at predetermined intervals to check for dye loss using a spectrophotometer. The percentage of methylene blue (MB) dye removed from the aqueous solution was determined using the following equation:

$$\text{Degradation efficiency} = \frac{C_0 - C}{C_0} \times 100\%$$

where C_0 is the initial concentration of methylene blue dye and C is the methylene blue dye concentration after a specific time.

3. Characterization

Ultraviolet-visible spectroscopy was used to validate the creation of the copper nanoparticles on a Jasco V-550 spectrophotometer, which possessed a size in the range of 300–700 nm. Fourier transform infrared spectroscopy analysis was performed in the range of 400–4000 cm^{-1} to identify the biomolecules present in the leaf extract, which reduced the copper ions. Here, the sample was ground with KBr to produce a pellet after centrifuging it at 9500 rpm for 20 min and drying in a hot air oven. Subsequently, the pellet was examined using a Jusco 5300 Fourier transform infrared spectrometer. X-Ray diffraction was performed on a Rigaku X-ray diffractometer (Miniflex, UK) at 40 kV with 2 s intervals at room temperature of 27 °C to investigate the crystalline structure of the copper nanoparticles. Scanning electron microscopy analysis was used to establish the morphology and mean particle size of the copper nanoparticles. A Supra Zeiss instrument with 1 nm resolution at 30 kV with a 20 mm Oxford Energy Dispersive X-ray detector was used to perform the scanning electron microscopy analysis. Energy Dispersive X-ray analysis was used to ascertain the elemental composition of the reaction mixture.

4. Statistical analysis

The GraphPad Prism software was used to perform the one-way analysis of variance (ANOVA) and Dunnett's multiple range test (Tukey's *post hoc* test) on the data. The data are presented for each experiment as the mean ± standard deviation (SD) from three experiments.

5. Result and discussion

5.1 X-ray diffraction

Using the XRD method, the microcrystalline structure of the greenly produced copper nanoparticles was further examined. All the peaks match copper, as shown in Fig. 3, with strong peaks at $2\theta = 32.1°$, 35.2°, 39.5°, 49.5°, 53.2°, 62.3°, 67.2°, 68.5° and 75.2°, corresponding to the (110), (002), (111), (202), (020), (113), (311), (220), and (222) planes, respectively. Ultimately, the data indicated the creation of the characteristic face-centred cubic symmetry. The sharp peaks further supported the production of copper nanoparticles with an extremely crystalline structure, which closely match the values of the face-centred cubic phase.[44]

Importantly, it is interesting to observe that the 2θ values of the synthesised copper nanoparticles match JCPDS No. 04-0836 as well as the Joint Committee for Powder Diffraction Standard (JCPDS). CuO, Cu_2O, and $Cu(OH)_2$ were found to be absent in the synthesised copper nanoparticles.[45] Additionally, the Debye–Scherrer equation was used to derive the average size of the copper nanoparticles, as follows:[46,47]

$$D = k\lambda/\beta \cos\theta$$

where D is the crystalline size of the nanoparticles and k is the Scherrer constant, which is 0.9, β is the full width at half-

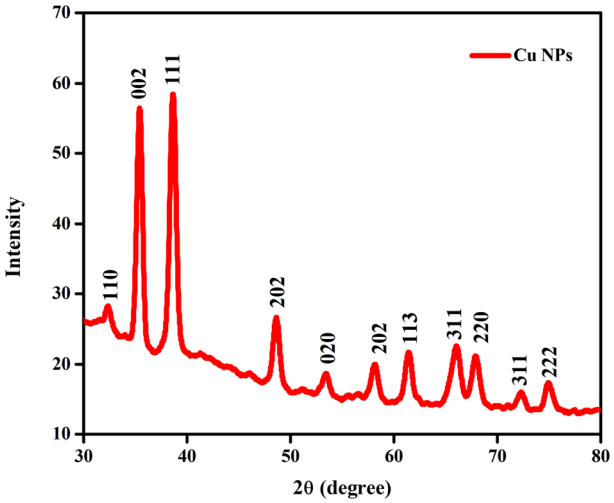

Fig. 3 X-ray diffraction pattern of copper nanoparticles, demonstrating their crystalline structure.

maximum (FWHM) of the primary intensity peak, λ is the X-ray wavelength (Cu Kα radiation wavelength, 1.5418 Å), and θ is the Bragg angle.[47] Subsequently, it was found the copper nanoparticles have an average crystalline size of 45 nm.

5.2 Ultraviolet-visible spectroscopy

Fig. 4(A) displays the UV-vis spectra of the green-mediated copper nanoparticles. Due to the simultaneous vibration of the metal nanoparticle free electrons in resonance with the light wave, metal nanoparticles feature a surface plasmon resonance (SPR) absorption band.[48]

An extract of *Emilia sonchifolia* leaves was used to manufacture copper nanoparticles in the wavelength range of 200–900 nm, which exhibited the characteristic absorption peak at 650 nm. As a result of the surface plasmon resonance (SPR) excitation trigger and the reduction of the substrates in the reaction mixture, the intensity of the colour change from blue to green indicated that copper nanoparticles were continually formed during incubation. Fig. 4(B) shows that the energy bandgap value of greenly synthesized Cu nanoparticles such as 1.83 eV. Additionally, it was discovered that as the particle size increased, the peak value gradually decreased. This is because the particles get opaque as their size increases.[49,50] The detection of larger particles or aggregation of small particles can be determined by using spectrophotometric analysis.[50]

5.3 Fourier transform infrared spectroscopy

To confirm the functional and active groups present in the bio-reduced copper nanoparticles created utilising aqueous leaf extract of *Emilia sonchifolia*, Fourier transform infrared spectroscopy analysis was also applied for their analysis. The NH and –COO groups in the *Emilia sonchifolia* leaf extract played a significant role in associating the active chemicals with copper, thereby equilibrating the biogenesis of the

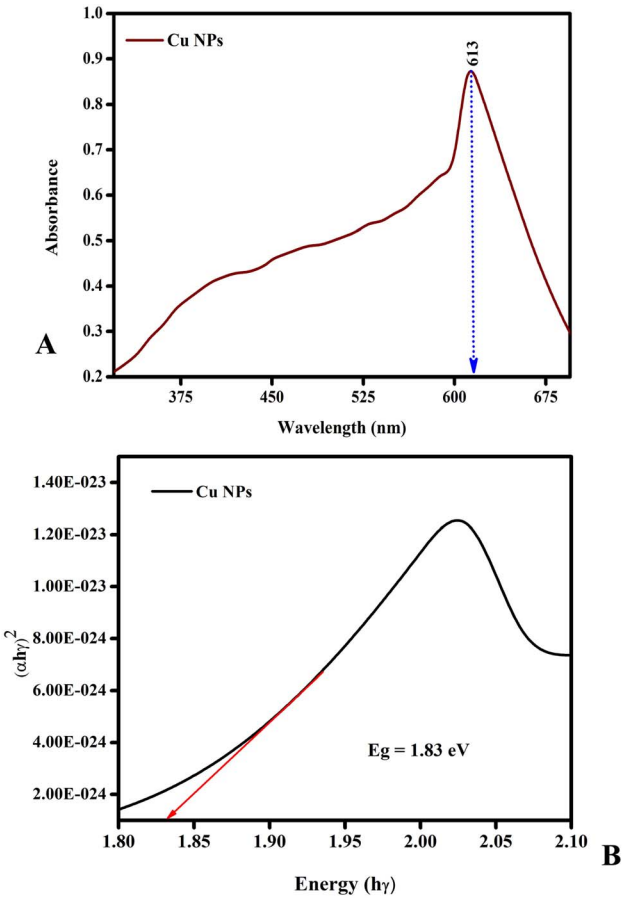

Fig. 4 UV-vis spectra of copper nanoparticles. The copper nanoparticle free electrons are in resonance with the light wave, and thus they feature a surface plasmon resonance (SPR) absorption band. (A) represent greenly synthesized Cu nanoparticles. (B) represent the band gap of greenly synthesized Cu nanoparticles.

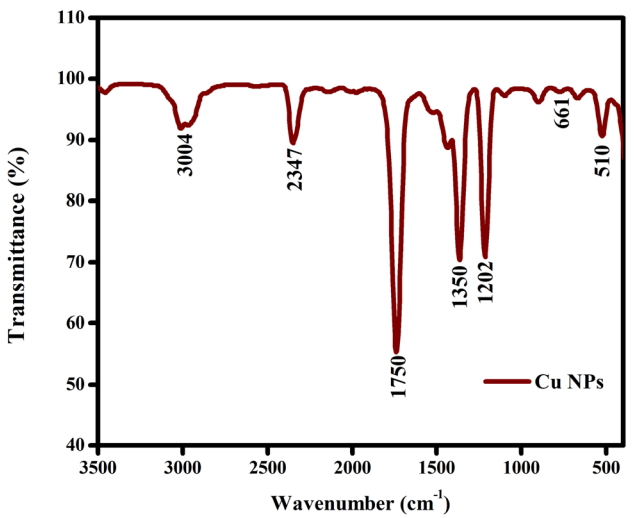

Fig. 5 Fourier transform infrared spectrum of copper nanoparticles. The functional groups appear to play a significant role in the creation of the copper nanoparticles.

Table 1 Vibrational modes of the functional groups in the copper nanoparticles

Wavenumber	Functional group
510 cm^{-1}	Copper vibration stretching bonds
661 cm^{-1}	Copper vibration stretching bonds
1202 cm^{-1}	C–C and C–O stretching
1350 cm^{-1}	CO–NH (amine group) stretching
1750 cm^{-1}	C=N bonds
2347 cm^{-1}	C=N bonds
3004 cm^{-1}	O–H and N–H bond stretching

nanoparticles, according to a prior publication in the Fourier transform infrared spectra of copper nanoparticles.[51,52]

The Fourier transform infrared spectroscopy analysis was carried out in the wavenumber range of 4000 to 500 cm^{-1}. The spectrum of the synthesised copper nanoparticles, as shown in Fig. 5, show bands located at 510 cm^{-1}, 661 cm^{-1}, 1202 cm^{-1}, 1350 cm^{-1}, 1750 cm^{-1}, 2347 cm^{-1}, and 3004 cm^{-1}. The O–H and N–H bond stretching vibrations correspond to the large peak located at 3004 cm^{-1}. The compounds with C=N bonds have tiny peaks at 2347 cm^{-1} and 1750 cm^{-1}, which are stretching vibrations. The sharp peak at 1350 cm^{-1} indicates the presence of amide, which may be due to the biomolecules in the *Calotropis* floral extract.[52] The copper vibrations cause smaller peaks to appear in the infrared spectrum at low frequencies below 700 cm^{-1}, such as 661 cm^{-1} and 510 cm^{-1}. Given that they supply the reducing groups that aid in the production of nanoparticles, the functional groups appear to play a significant role in the creation of the copper nanoparticles (Table 1).

5.4 Scanning electron microscopy-energy dispersive X-ray

SEM images were used to examine the morphology of the green copper nanoparticles created utilising the aqueous leaf extract of *Emilia sonchifolia* (Fig. 6). The spherical shape of the copper nanoparticles was confirmed, which were clumped together, similar to earlier reports on the synthesis of copper nanoparticles mediated by extracts of the *Magnolia champaca* plant.[53]

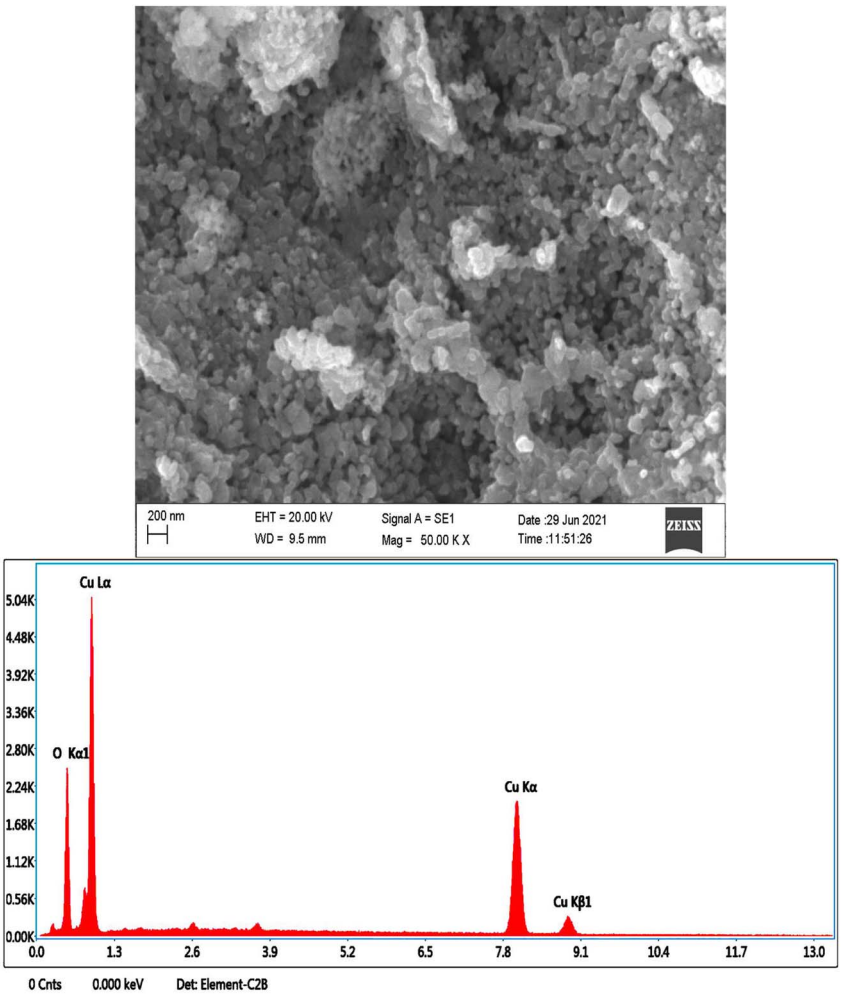

Fig. 6 Scanning electron microscopy-energy dispersive X-ray image of copper nanoparticles. SEM images were used to examine the morphology of the greenly produced copper nanoparticles. The copper nanoparticles subjected to energy dispersive X-ray investigation and the produced copper nanoparticles were clean and free of contaminants.

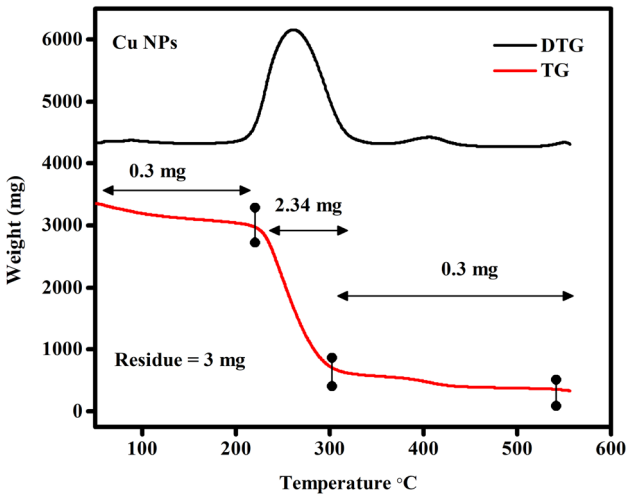

Fig. 7 Thermogravimetric and derivative thermogravimetric analysis of copper nanoparticles, with the derivative thermogravimetric analysis curve showing exothermic peaks at the same temperature range corresponding to the loss of mass observed in the thermogravimetric analysis.

Similarly, Vanaja *et al.* first reported on the aggregation of nanoparticles when they used *Morinda tinctoria* leaf extract to reduce copper ions.[54] Copper and oxygen elements were found to be present in the copper nanoparticles that were subjected to energy dispersive X-ray investigation (Fig. 6). Fig. 6 shows that the produced nanoparticles were clean and free of any contaminants.

5.5 Thermogravimetric analysis

Thermogravimetry (TG) is a technique that measures the mass of a sample against time or temperature.[55,56]

The thermogravimetric analysis was performed after the thermal disintegration of the copper nanoparticle powder. Fig. 7 depicts the thermogravimetric analysis (TGA) and derivative thermogravimetric analysis (DTG). The thermogravimetric analysis curve illustrates two major stages of weight loss. In addition to water and carbon dioxide evolution across the full weight loss range, in the first stage, approximately 0.3 mg weight loss occurred between 100 °C and 200 °C, corresponding to the loss of the groups on the surface of the material. In the second and main stage, approximately 2.39 mg weight loss occurred between 200 °C and 500 °C, which is attributed to the loss of organic compounds and other organic gases remaining after the pyrolysis. It can be observed that the derivative thermogravimetric analysis curve of the copper nanoparticles showed exothermic peaks at the same temperature ranges corresponding to the loss of mass observed in the thermogravimetric analysis. These peaks confirm the output of water and the broken chains. It was observed that there was no weight loss after 500 °C.

5.6 Copper nanoparticles induced hatching, mortality and malformation in zebrafish embryos and larvae

Numerous studies have shown that metal nanoparticles are hazardous to zebrafish eggs and larvae.[57–60]

The mortality of zebrafish embryos and larvae exposed to different concentrations of copper nanoparticles was determined at specific periods. As shown in Fig. 8 and 9, both the control and 10 μL of copper nanoparticles exhibited almost no toxicity to the zebrafish embryos or larvae. Compared with the control group, both 20 and 40 μL mL^{-1} of copper nanoparticles showed significant effects on mortality in the zebrafish embryos, which demonstrated toxicity, killing 55% and 80%, respectively, of the zebrafish embryos at 96 hpf. Consequently, at 96 hpf, the LC_{50} was calculated for all the concentrations. However, the 80 μL mL^{-1} copper nanoparticle-treated groups showed 100% mortality at 72 hpf. The hatching rates of the zebrafish embryos exposed to various concentrations of copper nanoparticles at early embryonic stages are shown in Fig. 8 and 9. During the normal condition, the zebrafish embryos had a hatching period comparable to that of the control group and 10–20 μL mL^{-1} copper nanoparticle-treated groups; however, at a concentration of 40–80 μL mL^{-1}, the copper nanoparticle-treated groups showed significant hatching delay. Also, 10 μL mL^{-1} of Cu NPs resulted in a lack of embryonic hatchability. Our data showed that exposure to copper nanoparticles caused developmental toxicity and a severe hatching retardation effect on the embryonic zebrafish, inducing malformation in the embryos. Subsequently, the embryos were exposed to 10–80 μL mL^{-1} of copper nanoparticles and the malformation was observed at 24–96 hpf (Fig. 8 and 9). The copper nanoparticle-treated group had significantly higher malformation rates than the control group. However, at a concentration of 80 μL mL^{-1}, the copper nanoparticle-treated embryos and larvae exhibited acute malformations and unhatched embryo (Fig. 9). At higher concentrations, the affected embryos were unable to hatch and eventually died (Fig. 8 and 9). Several malformation patterns including yolk-sac edema (YSE), eye malformation (EM), tail bent (TB) and spinal curvature bent (SB) were observed (Fig. 8). These observations showed that the unhatched embryonic phenotype was mainly induced by copper nanoparticles in the developing embryos. Similar malformations were also noted in zebrafish embryos after exposure to copper nanoparticles in earlier research.[61–65]

5.7 *In vitro*-anti-diabetic activity

The *in vitro* α-glucosidase inhibitory efficacy of the synthetic copper nanoparticles was tested in relation to a standard solution (Table 2 and Fig. 10). According to research, copper nanoparticles have a stronger anti-diabetic effect than *Emilia sonchifolia* leaf extract. The results showed that in the concentration range of 20–100 μL mL^{-1}, both copper nanoparticles and *Emilia sonchifolia* leaf extract produce dose-dependent inhibition of α-glucosidase enzyme activity. The IC_{50} values of anti-diabetic activity for the copper nanoparticles and *Emilia sonchifolia* leaf extract were 59.7 μL mL^{-1} and 46.1 μL mL^{-1}, respectively (Table 2). Additionally, the antidiabetic efficacy of the copper nanoparticles was marginally higher than that of the *Emilia sonchifolia* leaf extract, with the former inhibiting α-glucosidase by 92 ± 5%, while the latter inhibited it by 62.2 ± 5%. Thus, the copper nanoparticles should be further

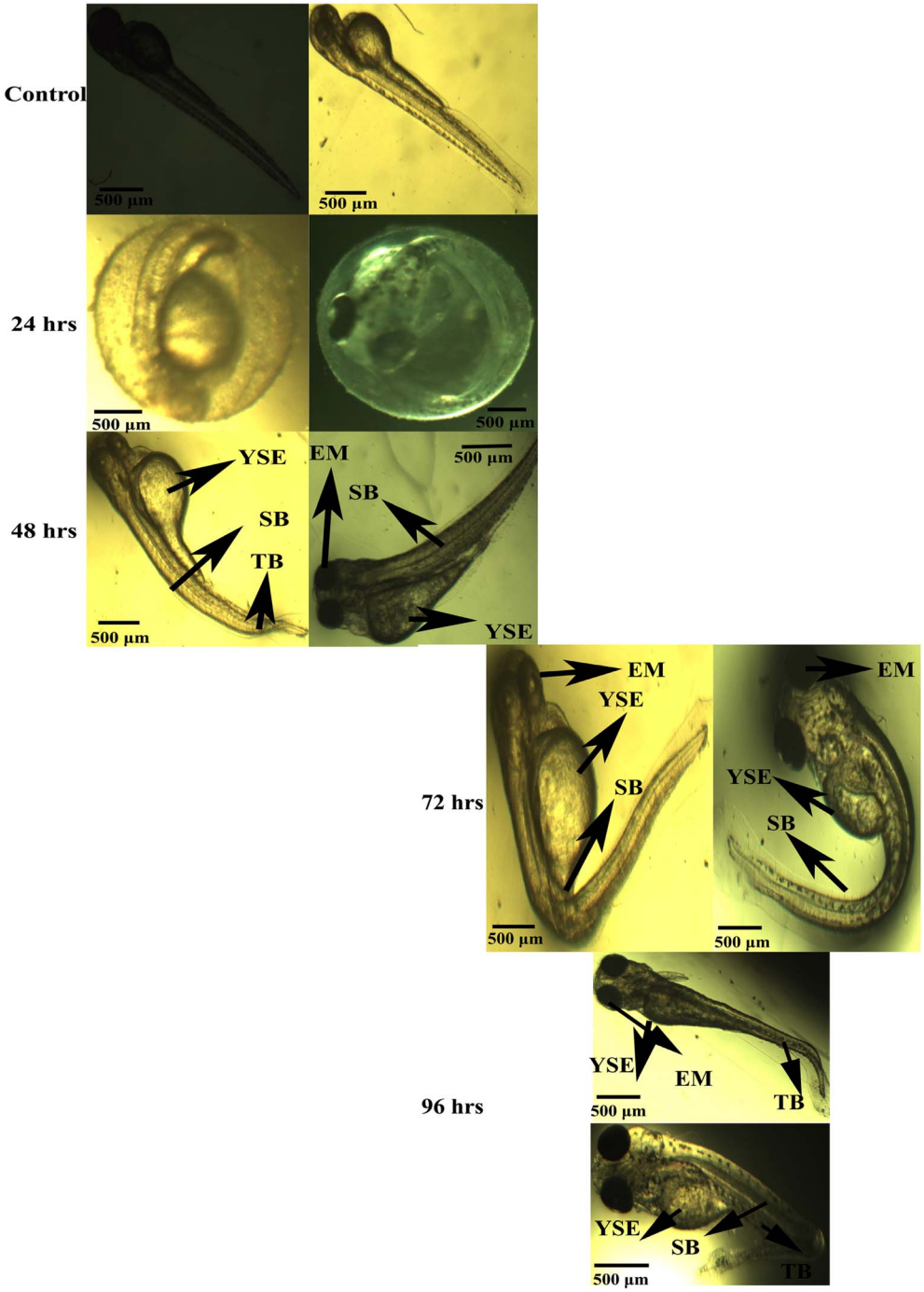

Fig. 8 Typical image of zebrafish embryos and larva exposed to copper nanoparticles. At 24 hpf, 48 hpf, 72 hpf, and 96 hpf, the control group displayed the predicted appearance. Eye malformation (EM), yolk sac edema (YSE), spinal curvature bent (SB), and tail bent (TB) are the major copper nanoparticle malformations, and each has its unique designation. Scale bar: 500 μm.

investigated for their anti-diabetic potential for therapeutic applications based on these results.

The previous reports demonstrating that copper nanoparticles can act as enzyme inhibitors with promising antidiabetic characteristics were further strengthened by the inhibition of α-glucosidase as well as murine intestinal α-glucosidase. *In vitro* investigations have shown that the copper ion and its complexes have significant α-glucosidase inhibitory action that is even stronger than acarbose, which is clinically employed.[66–71]

5.8 *In vitro* study on anti-inflammatory activity

The copper nanoparticles were tested for their anti-inflammatory action (inhibition of protein denaturation) at concentrations ranging from 10 to 80 μL mL^{-1}. Diclofenac sodium was used as

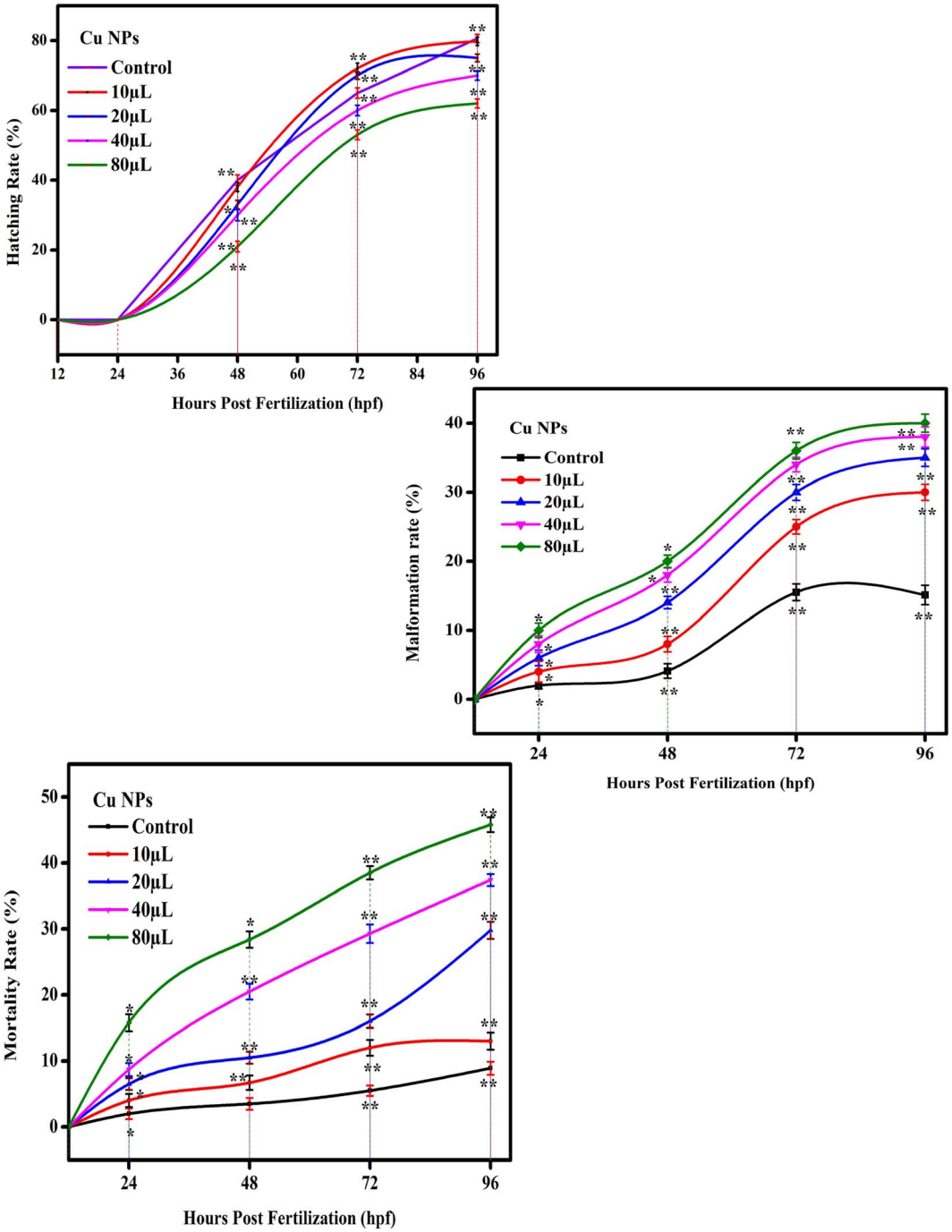

Fig. 9 Statistics for the copper nanoparticles is presented as mean ± standard deviation. The one-way analysis of variance (ANOVA) and Dunnett's Multiple range test (Tukey's *post hoc* test) were used to statistically analyse the data using statistical software. $p < 0.05$ and $p < 0.01$ are the respective standards for significance, denoted by "*" and "**", respectively.

a control material to compare the inhibitory effects of the prepared samples. The results showed that the two samples (*Emilia sonchifolia* and copper nanoparticles) inhibited egg albumin denaturation in a dose-dependent manner (Fig. 11). However, the copper nanoparticles exhibited higher anti-inflammatory activity than the *Emilia sonchifolia* samples. The IC_{50} values of anti-inflammatory activity for the copper nanoparticles and *Emilia sonchifolia* leaf extract were 239.3 μL mL^{-1} and 22 μL mL^{-1}, respectively (Table 2). Additionally, the anti-inflammatory efficacy of the copper nanoparticles was marginally higher than that of the *Emilia sonchifolia* leaf extract, where the former inhibited the protein denaturation of egg albumin by 30 ± 1%, while the latter inhibited it by 90.6 ± 9.2%. Earlier research found that the prevention of denaturation of egg albumin increased with an increase in the concentration of various nanostructures.[60,72,73] Previous research has shown that

Table 2 IC_{50} values for cytotoxicity, anti-inflammatory activity, and anti-diabetic activity

Activity	Concentration	Standard	*Emilia sonchifolia*	Copper nanoparticles
Anti-diabetic activity (α-glucosidase assay)	20 μL	42.6 ± 6.4	43 ± 15.7	65 ± 5
	40 μL	52 ± 7	48.3 ± 17.5	75 ± 5
	60 μL	63.6 ± 5.6	54 ± 19.6	85 ± 7.5
	80 μL	68.6 ± 5.6	60 ± 21.7	89 ± 6
	100 μL	67.6 ± 6.6	62 ± 22.5	92 ± 5
IC_{50} value		44.5	59.7	46.1
Anti-inflammatory activity	10 μL	60 ± 1	20 ± 1	34 ± 4.5
(protein denaturation-egg albumin)	20 μL	62 ± 1	22 ± 1	55 ± 5
	40 μL	64 ± 1	24 ± 1	80 ± 2.5
	60 μL	66 ± 1	26 ± 1	86.6 ± 5.8
	80 μL	69 ± 1	30 ± 1	90.6 ± 9.2
IC_{50} value		227.3	239.3	22.06
Human keratinocyte (HaCaT)	Control		74 ± 1	95 ± 1
cells cytotoxicity activity	10 μL		59 ± 1	90 ± 1
	20 μL		46 ± 1	74 ± 1
	40 μL		31 ± 1	59 ± 1
	60 μL		26 ± 1	46 ± 1
	80 μL		16 ± 1	31 ± 1
	100 μL		11 ± 1	26 ± 1
	120 μL		6 ± 1	16 ± 1
IC_{50} value			137.1	315.7
Human breast cancer (MCF- 7)	Control		75 ± 4	91 ± 3.6
cells cytotoxicity activity	10 μL		61 ± 4.7	87 ± 2.5
	20 μL		45 ± 4.1	75 ± 3.5
	40 μL		35 ± 2.5	59 ± 3
	60 μL		26 ± 2.5	51 ± 4
	80 μL		16 ± 2.5	45 ± 3
	100 μL		13 ± 3.5	30 ± 3.5
	120 μL		7 ± 2.5	21 ± 3.6
IC_{50} value			160	596.5

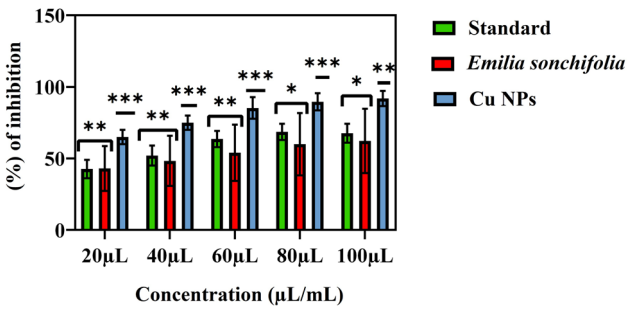

Fig. 10 Graph demonstrating the anti-diabetic activity of the copper nanoparticles. Data from three replicates are provided as the mean ± standard deviation. Using the Prism software, the data were statistically analysed using one-way analysis of variance (ANOVA) and Dunnett's multiple range test (Tukey's *post hoc* test). The statistical significance symbols "*", "**" and "***" stand for $p < 0.05$, $p < 0.01$ and $p < 0.005$, respectively.

protein denaturation, particularly of blood proteins such as albumin, is the primary cause of rheumatoid arthritis and inflammation.[65,74,75] Protein denaturation is the process by which proteins lose their tertiary and secondary structure as a result of external stress caused by physical or chemical agents such as heat shock. Protein denaturation is well known to result in the loss of biological function.[76]

5.9 *In vitro* study of cytotoxicity

The outcome of cytotoxicity tests on different cell lines, *i.e.*, human keratinocyte (HaCaT) and human breast cancer cells (MCF-7), using *Emilia sonchifolia* leaf extract and green-mediated copper nanoparticles showed that both the leaf extract and nanoparticles are hazardous to the cancerous cell lines but not to the normal cell lines (Fig. 12A and B), respectively. Fig. 12A demonstrates that at concentrations of 10–120

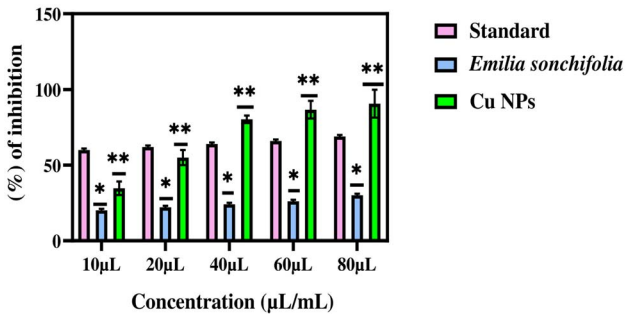

Fig. 11 Graph demonstrating the anti-inflammatory activity of the copper nanoparticles. Data from three replicates are represented as mean ± standard deviation. Using GraphPad Prism software, the data were statistically analysed using one-way analysis of variance (ANOVA) and Dunnett's multiple range test (Tukey's *post hoc* test). Statistical significance "*" and "**" stand for $p < 0.05$ and $p < 0.01$, respectively.

μL mL^{-1}, the cytotoxicity of the copper nanoparticles and the extract against the human breast cancer cell (MCF-7) tumor cell line was 80% and 52%, respectively. Fig. 12B reveals that following 72 h exposure to the synthetic leaf extract, the highest cell death measured in the cultivated human keratinocyte (HaCaT) cells was only 35%. When the concentration of copper nanoparticles was between 10 and 120 μL mL^{-1}, the human keratinocyte (HaCaT) cells were 60% more susceptible to cytotoxicity. Finally, as a result of the *in vitro* cytotoxicity, with an increase in concentration, the viability of the cancer cells decreased. Numerous studies conducted to date have demonstrated that phytochemical substances are harmless to healthy cells but hazardous to malignant cells.[77–82] As has already been established, the leaf extract is a rich source of phytochemicals, which account for its anticancer property seen in this study. Alternatively, the copper nanoparticles with increased activity could easily penetrate cells, interact with the cell components, and affect the cell regulatory pathways because of their high surface to volume ratio. It has been hypothesised that copper nanoparticles interact with mitochondria and the operation of the electron transport chain in cells, increasing the level of reactive oxygen species.[82–85] Consequently, the principal mechanism through which copper nanoparticles are hazardous to cells is the oxidative stress caused by reactive oxygen species. Given that cancerous cells have an abnormal metabolism and a high rate of proliferation, they are more vulnerable. Thus, the effect of the copper nanoparticles against cancerous cells occurs as a result of the high uptake of the nanoparticles by these cells. This result is good agreement with the data in the literature, which report the concentration-dependent toxicity of nanoparticles, particularly at lower levels.[83,86–88]

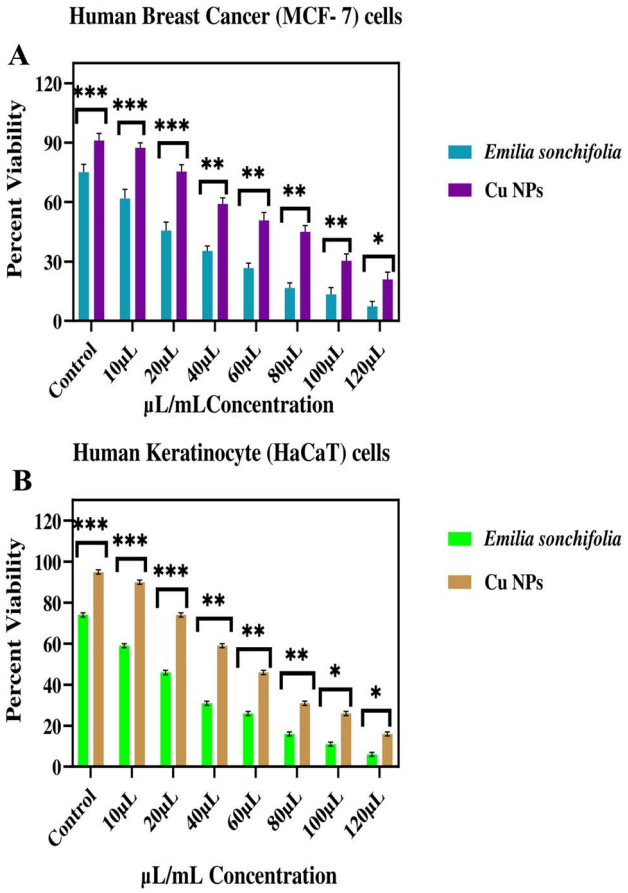

Fig. 12 Graph showing cytotoxicity of copper nanoparticles. Data from three replicates are provided as mean ± standard deviation. (A) *In vitro* cytotoxicity (cell viability) on human breast cancer (MCF-7) cells following the administration of various quantities of copper nanoparticles and plant extract (*Emilia sonchifolia*). (B) *In vitro* cytotoxicity (cell viability), as measured on human keratinocytes (HaCaT) cells, which are healthy human keratinocytes, following exposure to various quantities of copper nanoparticles and plant extract (*Emilia sonchifolia*). Using the GraphPad Prism software, the data were statistically analysed using one-way analysis of variance (ANOVA) and Dunnett's multiple range test (Tukey's *post hoc* test). Statistical significance "*" and "**" stand for $p < 0.05$ and $p < 0.01$, respectively.

5.10 Antibacterial activity

Due to the enhanced antibacterial activity of nanomedicine, it is widely applied.[89,90] Fig. 13 demonstrates that the antibacterial of the copper nanoparticles against different bacteria.

The agar well diffusion method was used to test the antibacterial activity of the green-generated copper nanoparticles, which showed a large zone of inhibition against *E. coli*, *Staphylococcus aureus*, *Pseudomonas*, *Enterobacter* and *Bacillus*. Occasionally, a smaller zone of inhibition was produced at a lower concentration, showing the effect of the concentration of copper nanoparticles on the zone of inhibition. The zone of inhibition was determined in mm (millimetres), demonstrating that the effective prevention of bacterial growth was accomplished with the use of the copper nanoparticles.[91–93]

5.11 Photocatalytic activity

5.11.1 Mechanism of photocatalytic activity. As shown in Fig. 14, the breakdown of the methylene blue dye is a ultraviolet light-dependent process. During this process, a positive hole (h^+) is promoted to the valence band, and the material is then exposed to ultraviolet radiation to excite the valence electrons and permit them to move from the valence band to the conduction band. The positive holes and free electrons interact with the adsorbed water molecules on the photocatalyst surface to form hydroxy (OH) radicals, while free electrons convert dissolved oxygen into superoxide anion oxygen (O_2) radicals. Subsequently, these light-generated radicals disassemble the dye molecules into simpler molecules such as carbon dioxide (CO_2) and water (H_2O).[94,95]

$$\text{Cu NPs} + h\nu(\text{UV}) \rightarrow \text{Cu NPs}\ (e^-(\text{CB}) + h^+(\text{VB}))$$

$$H_2O + h^+(\text{VB}) \rightarrow OH^\cdot + H^+$$

$$(O_2^-)\cdot O_2 + e^-(\text{CB}) \rightarrow O_2^{-\cdot}$$

$$(OH^\cdot)\cdot O_2^{-\cdot} + H^+ \rightleftarrows HOO^\cdot$$

$$2HOO^\cdot \rightarrow H_2O_2 + O_2$$

$$H_2O_2 \rightarrow 2OH^\cdot$$

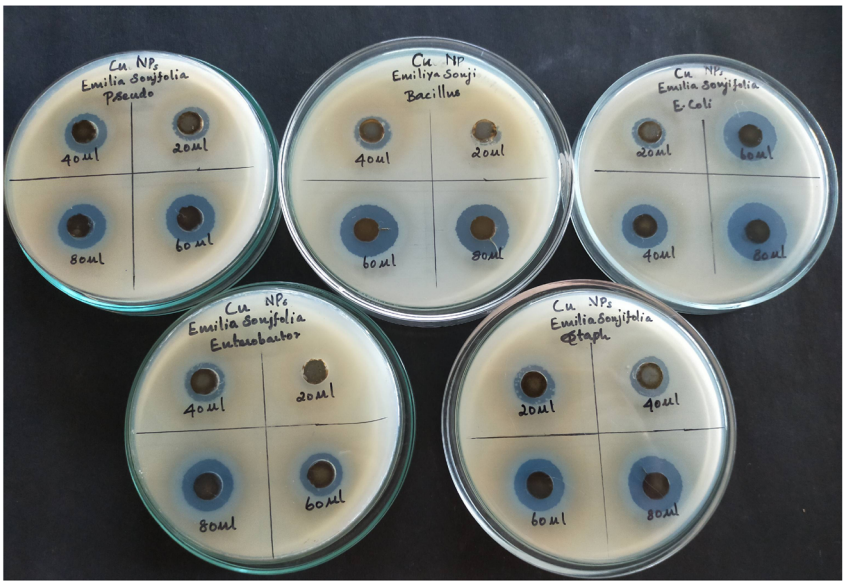

Fig. 13 Antibacterial activity of copper nanoparticles synthesized using *Emilia sonchifolia* leaf extract. The agar well diffusion method was used to test their antibacterial activity.

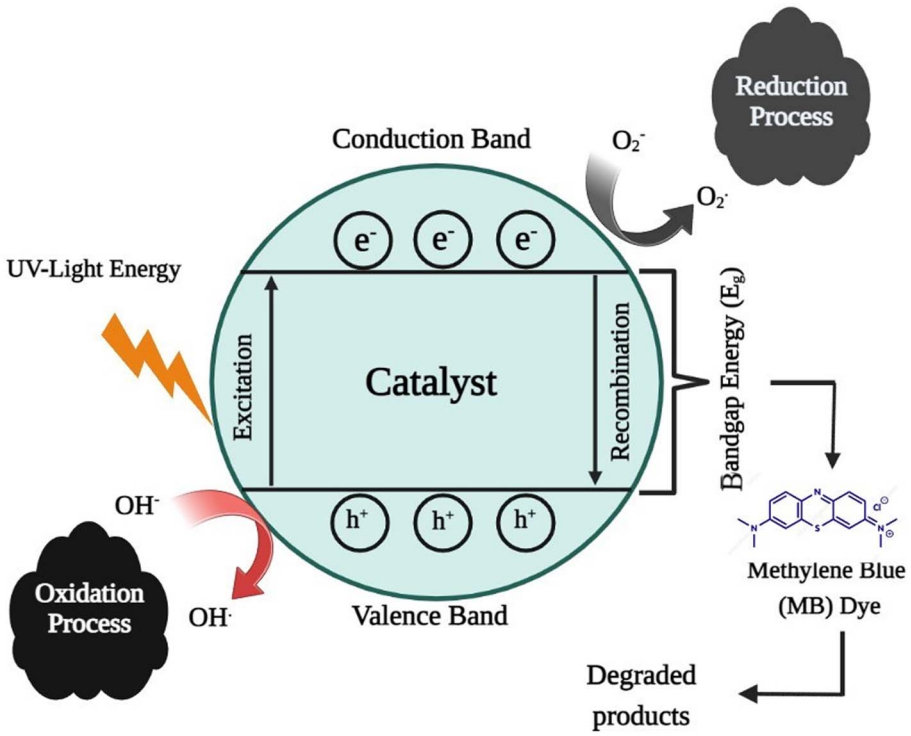

Fig. 14 Reaction mechanisms for the degradation of methylene blue.

$$\text{Methylene blue dye} + OH^{\bullet} \rightarrow CO_2 + H_2O \text{ (dye intermediates)}$$

$$\text{Methylene blue dye} + h^+(VB) \rightarrow \text{oxidation products}$$

$$\text{Methylene blue dye} + e^-(CB) \rightarrow \text{reduction products}$$

$$\text{Methylene blue dye} + h\nu \rightarrow \text{methylene blue dye}^*$$

$$\text{Methylene blue dye}^* + \text{Cu NPs} \rightarrow \text{methylene blue dye}+ + \text{Cu NPs}^-$$

5.11.2 Photocatalytic activity of copper nanoparticles. Recyclability and reusability are two main properties for evaluating the performance of a catalyst bed in industrial catalytic

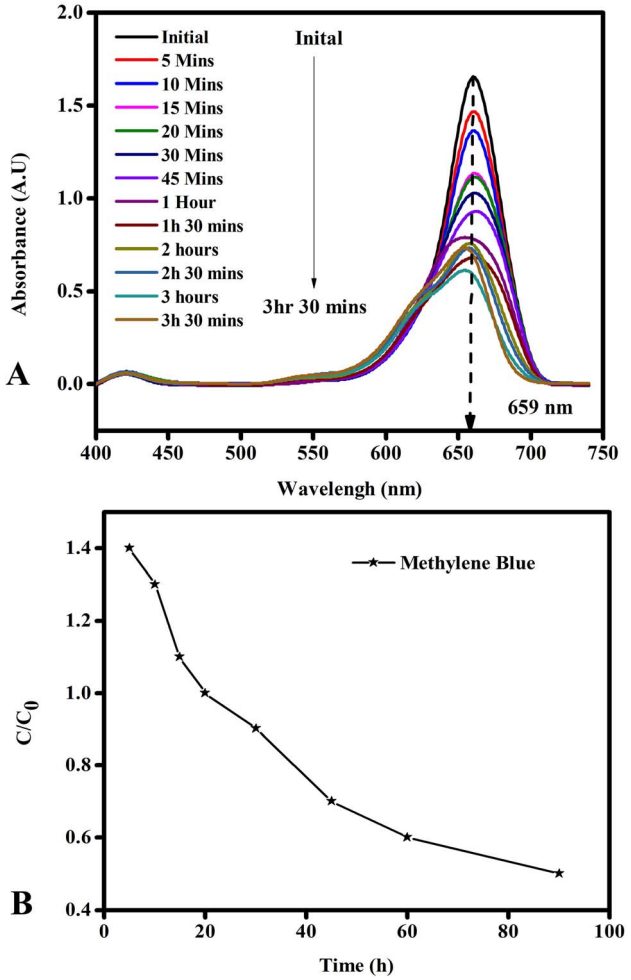

Fig. 15 Photocatalytic activity of copper nanoparticles: (A) absorbance of copper nanoparticles with time and (B) degradation of dye by copper nanoparticles. The complete degradation of methylene blue was achieved using the copper nanoparticles as a nanocatalyst.

degradation applications.[95] In this work, we evaluated the properties of the copper nanoparticles through a simple experiment involving the repeated degradation of dyes. The experimental process of copper nanoparticles of methylene blue is shown in Fig. 15. The reactions were carried out with a fixed amount of reactants and catalyst (0.01 g copper nanoparticles). Fig. 15 shows the time required for the complete degradation of methylene blue by using the copper nanoparticles as a nanocatalyst. The degradation performance of the copper nanoparticles decreased slightly in the continuous cycle due to the loss of the composite material during the recovery/washing process. The active sites of the copper nanoparticles may have also been blocked by the reaction product during the reduction process.[96,97] The result showed that the copper nanoparticles can maintain high catalytic activity with a high frequency turnover.

6. Conclusion

In conclusion, a green route yielded copper nanoparticles. The green-mediated synthesis of the copper nanoparticles was analyzed using different instrumental techniques during the synthesis process. The *in vivo* toxicity in zebrafish and several biological *in vitro* activities of the copper nanoparticles were investigated. The results revealed that compared to the leaf extract, the green-prepared copper nanoparticles (*Emilia sonchifolia*) displayed higher levels of antidiabetic and anti-inflammatory activities. Human keratinocyte cancer cells (HaCaT) and human breast cancer cells (MCF-7) showed increased sensitivity to the greenly produced copper nanoparticles. It was interesting to note that the green copper nanoparticles were less harmful to zebrafish embryos. This study provides a low-cost, environmentally acceptable method for the green synthesis of copper nanoparticles with potential for use in the pharmaceutical industry.

Data availability

The corresponding author will provide the following information from the manuscript upon reasonable request.

Funding

The authors affirm that they have not received any money for their research.

Consent for publication and involvement

All individuals taking part in the study gave their informed permission.

Coding accessibility

Not relevant.

Author contributions

The authors collaborated to finish this piece. Vainath Praveen Sankara Narayanan was the author and researcher of the study. Author Sabeena Gabrial Kathirason wrote the original draught of the manuscript. Author Pushpalakshmi Elango and Rajaduraipandian Subramanian oversaw the statistical analysis, investigation, analyses, and rectification. The accompanying author Annadurai Gurusamy, who also oversaw the aforementioned study, established the experimental effort's technique. All authors read the final draught and gave their consent.

Conflicts of interest

The authors affirm that they have no competing interests with this investigation.

Acknowledgements

In order to complete this study, S. Vainath Praveen (Reg. No. 22214012051020) appreciates the Sri Paramakalyani Centre for

Excellence in Environmental Science at Manonmaniam Sundaranar University in Alwarkurichi, India.

References

1 K. Parveen, V. Banse and L. Ledwani, Green synthesis of nanoparticles: their advantages and disadvantages, *AIP Conf. Proc.*, 2016, **1724**, 020048.
2 M. Shah, D. Fawcett, S. Sharma, S. Tripathy and G. Poinern, Green synthesis of metallic nanoparticles *via* biological entities, *Materials*, 2015, **8**(11), 7278–7308.
3 I. M. Chung, A. A. Rahuman, S. Marimuthu, A. V. Kirth, K. Anbarasan, P. Padmini and G. Rajakumar, Green synthesis of copper nanoparticles using Eclipta prostrate leaves extract and their antioxidant and cytotoxic activities, *Exp. Ther. Med.*, 2017, **14**(1), 14–18.
4 G. Geoprincy, B. N. Vidhyasrr, U. Poonguzhali, N. Nagendra Gandhi and S. Renganathan, A review on green synthesis of silver nano particles, *Asian J. Pharm. Clin. Res.*, 2013, **6**, 8–12.
5 I. Ocsoy, D. Tasdemir, S. Mazicioglu, C. Celik, A. Katı and F. Ulgen, Biomolecules incorporated metallic nanoparticles synthesis and their biomedical applications, *Mater. Lett.*, 2018, **212**, 45–50.
6 M. Batoool and B. Masood, Green synthesis of copper nanoparticles using Solanum Lycopersicum (tomato aqueous extract) and study characterization, *J. Nanosci. Nanotechnol. Res.*, 2017, **1**, 1–5.
7 P. Padma, & S. Banu and S. Kumari, Studies on green synthesis of copper nanoparticles using Punica granatum, *Annu. Res. Rev. Biol.*, 2018, **23**(1), 1–10.
8 M. Nasrollahzadeh, S. M. Sajadi and M. Khalaj, Green synthesis of copper nanoparticles using aqueous extract of the leaves of Euphorbia esula L and their catalytic activity for ligand-free Ullmann-coupling reaction and reduction of 4-nitrophenol, *RSC Adv.*, 2014, **4**(88), 47313–47318.
9 D. A. Jamdade, D. Rajpali, K. A. Joshi, R. Kitture, A. S. Kulkarni, V. S. Shinde, J. Bellare, K. R. Babiya and S. Ghosh, Gnidia glauca - and Plumbago zeylanica – mediated synthesis of novel copper nanoparticles as promising antidiabetic agents, *Adv. Pharmacol. Sci.*, 2019, 1–11.
10 N. Elisma, A. Labanni, E. Emriadi, Y. Rilda, M. Asrofi and S. Arief, Green synthesis of copper nanoparticles using Uncaria gambir roxb. leaf extract and its characterization, *Rasayan J. Chem.*, 2019, **12**(4), 1752–1756.
11 M. Ahmed, Q. Y. Usman, Y. Q. Liu, B. Shen and H. L. Yu, Cong, Plant mediated synthesis of copper nanoparticles by using Camelia sinensis leaves extract and their applications in dye degradation, *Ferroelectrics*, 2019, **549**(1), 61–69.
12 P. E. Das, I. A. Abu-Yousef, A. F. Majdalawieh, S. Narasimhan and P. Poltronieri, Green synthesis of encapsulated copper nanoparticles using a hydroalcoholic extract of Moringa oleifera leaves and assessment of their antioxidant and antimicrobial activities, *Molecules*, 2020, **25**(3), 555.
13 O. Długosz, J. Chwastowski and M. Banach, Hawthorn berries extract for the green synthesis of copper and silver nanoparticles, *Chem. Pap.*, 2020, **74**, 239–252.
14 E. A. Mohamed, Green synthesis of copper & copper oxide nanoparticles using the extract of seedless dates, *Heliyon*, 2020, **6**(1), e03123.
15 J. J. Mohindru and U. K. Garg, Green synthesis of copper nanoparticles using tea leaf extract, *Int. J. Eng. Sci. Res. Technol.*, 2017, **6**(7), 307–311.
16 S. D. Ashtaputrey, P. D. Ashtaputrey and N. Yelane, Green synthesis and characterization of copper nanoparticles derived from Murraya koenigii leaves extract, *Int. J. Chem. Pharm. Sci.*, 2017, **10**(3), 1288–1291.
17 V. Kulkarni and P. Kulkarni, Synthesis of copper nanoparticles with Aegle marmelos leaf extract, *J. Nanosci. Nanotechnol.*, 2014, **8**(10), 401–404.
18 S. L. Nair and R. N. Chopra, in *Glossary of Indian Medicinal Plants*. National Institute of Science and Communication, New Delhi, 1996, p. 107.
19 C. P. Khare, *Emilia sonchifolia* (L.) DC, *Indian Medicinal Plants: An Illustrated Dictionary*. Springer-Verlag, Berlin Heidelberg, 2007, p. 01.
20 G. K. Dash, M. S. Abdullah and R. Yahaya, Traditional Uses, Phytochemical And Pharmacological Aspects of Emilia Sonchifolia (L.) DC, *Int. J. Res. Ayurveda Pharm.*, 2015, **6**(4), 551–556, DOI: 10.7897/2277-4343.064103.
21 K. Satyavathi, S. Satyavani, T. S. N. Padal and S. B. Padal, Ethnomedicinal plants used by primitive tribal of Pedabayalu Mandalam, Visakhapatnam district, A. P, India, *Int. J. Ethnobiol. Ethnomedicine*, 2014, **1**(25), 1–7.
22 D. Gayathri Devi, Y. Lija, T. R. Cibin, P. G. Biju, V. Gayathri Devi and A. Abraham, Evaluation of protective effects of *Emilia sonchifolia Linn*. (DC.) on perchlorate-induced oxidative damage, *J. Biol. Sci.*, 2006, **6**, 887–892.
23 S. K. Adesina, Studies on a Nigerian herbal anticonvulsant recipe, *Int. J. Crude Drug Res.*, 1982, **20**, 93–100.
24 L. S. Gill, H. G. K. Nyawuame, E. I. Esezebor and I. S. Osagie. *Nigerian Folk Medicine: Practices and believes of Esan people. Benin (Nigeria)*: University of Benin Press, Benin, 1993, pp. 1–20.
25 R. G. Saratale, I. Karuppusamy, G. D. Saratale, A. Pugazhendhi, G. Kumar, Y. Park, G. S. Ghodake, R. N. Bharagava, J. R. Banu and H. S. Shin, A comprehensive review on green nanomaterials using biological systems: Recent perception and their future applications, *Colloids Surf.*, 2018, **170**, 20–35.
26 A. Tamilvanan, B. Kulendran, K. Ponappa and B. Kumar, Copper Nanoparticles Synthetic Strategies Properties and Multifunctional Application, *Int. J. Nanosci.*, 2014, **13**(2), 1430001.
27 M. B. Gawande, A. Goswami, F. X. Felpin, T. Asefa, X. Huang, R. Silva, X. Zou, R. Zboril and R. S. Varma, Cu and Cu-Based Nanoparticles: Synthesis and Applications in Catalysis, *Chem. Rev.*, 2016, **116**, 3722.
28 Z. Issaabadi, M. Nasrollahzadeh and S. M. Sajadi, Green synthesis of the copper nanoparticles supported on

bentonite and investigation of its catalytic activity, *J. Cleaner Prod.*, 2017, **142**, 3584–3591.

29 Z. Ismail, *et al.*, Prevalence of depression in patients with mild cognitive impairment: A systematic review and meta-analysis, *JAMA Psychiatry*, 2017, **74**(1), 58–67.

30 K. Saranyaadevi, V. Subha, R. S. Ernest Ravindran and S. Renganathan, Synthesis and Characterization of Copper Nanoparticle using Capparis Zeylanicaleaf Extract, *Int. J. ChemTech Res.*, 2014, **6**(10), 4533–4541.

31 P. Krishnamoorthy and T. Jayalakshmi, Preparation, characterization and synthesis of silver nanoparticles by using *Phyllanthus niruri* for the antimicrobial activity and cytotoxic effects, *J. Chem. Pharm. Res.*, 2012, **4**(11), 4783–4794.

32 I. Subhankari and P. L. Nayak, Antimicrobial Activity of Copper Nanoparticles Synthesised by Ginger (*Zingiber officinale*) Extract, *World J. Nano Sci. Technol.*, 2013, **2**(1), 10–13.

33 OECD, *Test No. 236: Fish Embryo Acute Toxicity (FET) Test*, OECD Publishing, Paris, 2013.

34 J. Santhoshkumar and V. Kumar, Green Synthesis of Copper Oxide Nanoparticles from Magnolia Champaca Floral Extract and its Antioxidant & Toxicity Assay using Danio Rerio, *Int. J. Recent. Technol. Eng.*, 2020, **8**(5), 5444–5449.

35 N. B. Abramenko, T. B. Demidova, E. V. Abkhalimov, B. G. Ershov, E. Yu. Krysanov and L. M. Kustov, Ecotoxicity of different-shaped silver nanoparticles: Case of zebrafish embryos, *J. Hazard. Mater.*, 2018, **347**, 89–94.

36 D. Selvan, S. Arumai, S. Shobana and A. Murugesan, kalilur Rahiman, Antidiabetic Activity of Phytosynthesized Ag/CuO Nanocomposites Using Murraya Koenigii and Zingiber Officinale Extracts, *Research Square*, 2022, **10**(2), 02–03.

37 P. Dey, P. Chatterjee, S. Chandra and S. Bhattacharya, Comparative *in vitro* evaluation of anti-inflammatory effects of aerial parts and roots from Mikania scandens, *J. Adv. Pharm. Technol. Res.*, 2011, **1**, 271–277.

38 S. Chandra, P. Chatterjee, P. Dey and S. Bhattacharya, Evaluation of anti-inflammatory effect of ashwagandha: a preliminary study in vitro, *Pharmacogn. J.*, 2012, **4**(29), 47–49.

39 E. Mostaghasi, A. Zarepour and A. Zarrabi, Folic acid armed Fe_3O_4-HPG nanoparticles as a safe nano vehicle for biomedical theranostics, *J. Taiwan Inst. Chem. Eng.*, 2018, **82**, 33–41.

40 Z. Assadi, G. Emtiazi and A. Zarrabi, Hyperbranched polyglycerol coated on copper oxide nanoparticles as a novel core-shell nano-carrier hydrophilic drug delivery model, *J. Mol. Liq.*, 2018, **250**, 375–380.

41 A. Zarrabi, M. A. Shokrgozar, M. Vossoughi and M. Farokhi, In vitro biocompatibility evaluations of hyperbranched polyglycerol hybrid nanostructure as a candidate for nanomedicine applications, *J. Mater. Sci.: Mater. Med.*, 2014, **25**(2), 499–506.

42 K. Ameta, P. Tak, D. Soni and S. C. Ameta, Photocatalytic decomposition of malachite green over lead chromate powder, *Sci. Rev. Chem. Commun.*, 2014, **4**(1), 38–45.

43 P. Koteeswari, S. Sagadevan, I. Fatimah, A. Kassegn Sibhatu, S. Izwan Abd Razak, E. Leonard and T. Soga, Green synthesis and characterization of copper oxide nanoparticles and their photocatalytic activity, *Inorg. Chem. Commun.*, 2022, **144**, 109851.

44 D. Zhou, A. I. Abdel-Fattah and A. A. Keller, Clay particles destabilize engineered nanoparticles in aqueous environments, *Environ. Sci. Technol.*, 2012, **46**(14), 7520–7526.

45 W. Yu, H. Xie, L. Chen, Y. Li and C. Zhang, Synthesis and Characterization of Monodispersed Copper Colloids in Polar Solvents, *Nanoscale Res. Lett.*, 2009, **4**(5), 465–470.

46 B. Malaikozhundan, B. Vaseeharan, S. Vijayakumar, R. Sudhakaran, N. Gobi and G. Shanthini, Antibacterial and antibiofilm assessment of Momordica charantia fruit extract coated silver nanoparticle, *Biocatal. Agric. Biotechnol.*, 2016, **8**, 189–196.

47 B. V. Jogiya, K. S. Chudasama, V. S. Thaker and M. J. Joshi, XRD, Thermal, Haemolysis and DNA Binding Studies of L-Arginine Functionalized Hydroxyapatite Nanoparticles, *J. Nanomed. Res.*, 2016, **3**(6), 00073.

48 P. Kouvaris, A. Delimitis, V. Zaspalis, D. Papadopoulos, S. A. Tsipas and N. Michailidis, Green synthesis and characterization of silver nanoparticles produced using Arbutus Unedo leaf extract, *Mater. Lett.*, 2012, **76**, 18–20.

49 E. G. Goh, X. Xu and P. Mccormick., The effect of particle size on the UV absorbance of Zinc Oxide nanoparticles, *Scr. Mater.*, 2014, **78–79**, 49–52.

50 T. Nakamura, Y. Herbani, D. Ursescu, B. Romeo, R. V. Dabu and S. Sato, Spectroscopic study of gold nanoparticle formation through high intensity laser irradiation of solution, *AIP Adv.*, 2013, **3**, 082101.

51 C. Krishnaraj, G. M. Young and S.-I. Yun, *In vitro* embryotoxicity and mode of antibacterial mechanistic study of gold and copper nanoparticles synthesized from Angelica keiskei (Miq.) Koidz. leaves extract, *Saudi J. Biol. Sci.*, 2022, **29**(4), 2552–2563.

52 A. Jayadev and N. Krishnan B, Green Synthesis of Copper Nanoparticles and its Characterization, *J. Sci. Res.*, 2021, **65**(01), 80–84.

53 D. Rehana, D. Mahendiran, R. S. Kumar and A. K. Rahiman, Evaluation of antioxidant and anticancer activity of copper oxide nanoparticles synthesized using medicinally important plant extracts, *Biomed. Pharmacother.*, 2017, **89**, 1067–1077.

54 M. Vanaja, K. Paulkumar, M. Baburaja, S. Rajeshkumar, G. Gnanajobitha, C. Malarkodi, M. Sivakavinesan and G. Annadurai, Degradation of Methylene Blue Using Biologically Synthesized Silver Nanoparticle, *Bioinorg. Chem. Appl.*, 2014, 742346–742354.

55 F. Jahantigh and M. Nazirzadeh, Synthesis and Characterization of TiO2 Nanoparticles with Polycarbonate and Investigation of its Mechanical Properties, *Int. J. Nanosci.*, 2017, **16**(05n06), 1750012.

56 A. Varughese, R. Kaur and P. Singh, Green Synthesis and Characterization of Copper Oxide Nanoparticles Using

Psidium guajava Leaf Extract, *IOP Conf. Ser.: Mater. Sci. Eng.*, 2020, **961**, 012011.
57 P. V. Asharani, Y. I. Lian, Z. Gong and S. Valiyaveettil, Toxicity of silver nanoparticles in Zebrafish models Nanotechnology, *Nanotechnology*, 2008, **19**(25), 255102.
58 X. Zhu, L. Zhu, Z. Duan, R. Qi, Y. Li and Y. Lang, Comparative toxicity of several metal oxide nanoparticle aqueous suspensions to Zebrafish (Danio rerio) early developmental stage, *J. Environ. Sci. Health, Part A: Toxic/Hazard. Subst. Environ. Eng.*, 2008, **43**, 278–284.
59 P. Karthiga, M. Ponnanikajamydeen, R. Samuel Rajendran, G. Annadurai and S. Rajeshkumar, Characterization and toxicology evaluation of zirconium oxide nanoparticles on the embryonic development of zebrafish, Danio rerio, *Drug Chem. Toxicoly.*, 2018, **42**(1), 104–111.
60 G. Sabeena, S. Rajaduraipandian, T. Manju, H. A. Alhadlaq, R. Mohan, G. Annadurai and M. Ahamed, In vitro antidiabetic and anti-inflammatory effects of Fe-doped CuO-rice husk silica (Fe-CuO-SiO2) nanocomposites and their enhanced innate immunity in zebrafish, *J. King Saud Univ., Sci.*, 2022, 102121.
61 W. Bai, W. Tian, Z. Zhang, X. He, Y. Ma, N. Liu and Z. Chai, Effects of copper nanoparticles on the development of zebrafish embryos, *J. Nanosci. Nanotechnol.*, 2010, **10**(12), 8670–8676.
62 N. Malhotra, T. R. Ger, B. Uapipatanakul, J. C. Huang, K. H. Chen and C. D. Hsiao, Review of Copper and Copper Nanoparticle Toxicity in Fish, *Nanomaterials*, 2020, **10**(6), 1126.
63 R. J. Griffitt, R. Weil, K. A. Hyndman, N. D. Denslow, K. Powers, D. Taylor and D. S. Barber, Exposure to Copper Nanoparticles Causes Gill Injury and Acute Lethality in Zebrafish (Danio rerio), *Environ. Sci. Technol.*, 2007, **41**, 8178–8186.
64 J. X. Liu, T. Zhang, H. J. Sun and J. X. Liu, Copper nanoparticles induce zebrafish intestinal defects *via* endoplasmic reticulum and oxidative stress, *Metallomics*, 2020, **12**, 12–22.
65 G. Sabeena, S. Rajaduraipandian, E. Pushpalakshmi, H. A. Alhadlaq, R. Mohan, G. Annadurai and M. Ahamed, Green and chemical synthesis of CuO nanoparticles: A comparative study for several *in vitro* bioactivities and *in vivo* toxicity in zebrafish embryos, *J. King Saud Univ., Sci.*, 2022, 102092.
66 Y. Wang, L. Ma, Z. Li, Z. Du, Z. Liu, *et al.*, Synergetic inhibition of metal ions and genistein on alpha-glucosidase, *FEBS Lett.*, 2004, **576**, 46–50.
67 J. Vanco, J. Marek, Z. Trávnícek, E. Racanská, J. Muselík, *et al.*, Synthesis, structural characterization, antiradical and antidiabetic activities of copper(II) and zinc(II) Schiff base complexes derived from salicylaldehyde and ß-alanine, *J. Inorg. Biochem.*, 2008, **102**, 595–605.
68 N. Yasumatsu, Y. Yoshikawa, Y. Adachi and H. Sakurai, Antidiabetic copper(II)-picolinate: impact of the first transition metal in the metallopicolinate complexes, *Bioorg. Med. Chem.*, 2007, **15**, 4917–4922.
69 Z. Jiao, J. Liu and S. Wang, Antioxidant activities of total pigment extract from blackberries, *Food Technol. Biotechnol.*, 2005, **43**, 97–102.
70 J. V. Hunt, R. T. Dean and S. P. Wolff, Hydroxyl radical production and autoxidative glycosylation. Glucose autoxidation as the cause of protein damage in the experimental glycation model of diabetes mellitus and ageing, *Biochem. J.*, 1988, **256**, 205–212.
71 S. Ghosh, P. More, R. Nitnavare, S. Jagtap, R. Chippalkatti, *et al.*, Antidiabetic and Antioxidant Properties of Copper Nanoparticles Synthesized by Medicinal Plant Dioscorea bulbifera, *J. Nanomed. Nanotechnol.*, 2015, **6**, 007.
72 M. V. Anoop and A. R. Bindu, In-vitro anti-inflammatory activity studies on Syzygium zeylanicum (L) DC leaves, *Int. J. Pharma Res. Rev.*, 2015, **4**, 18–27.
73 M. Govindappa, S. S. Naga, M. N. Poojashri, T. S. Sadananda and C. P. Chandrappa, Antimicrobial, antioxidant and *in vitro* anti-inflammatory activity of ethanol extract and active phytochemical screening of Wedelia trilobata (L.) Hitchc, *J. Pharmacogn. Phytother.*, 2011, **3**, 43–51.
74 C. Sangita, C. Priyanka, C. Protapaditya and B. Sanjip, Evaluation of anti-inflammatory activity of coffee against the denaturation of protein, *Asian Pac. J. Trop. Biomed.*, 2012, **2**(1), 178–180.
75 S. Krithika, K. L. Niraimathi, K. P. Arun, R. Narendran, K. Balaji and P. Brindha, In vitro antiinflammatory studies on silver nanoparticles synthesized from Centratherum punctatum Cass, *Int. J. Res. Ayurveda Pharm.*, 2016, **7**(2), 61–66.
76 G. Leelaprakash and M. S. Dass, In vitro anti-inflammatory activity of methanol extract of Enicostemma axilarre, *Int. J. Drug Dev. Res.*, 2011, **3**(3), 189–196.
77 A. Constantinou, G. D. Stoner, R. Mehta, K. Rao, C. Runyan and R. Moon, The dietary anticancer agent ellagic acid is a potent inhibitor of DNA topoisomerases in vitro, *Nutr. Cancer*, 1995, **23**(2), 121–130.
78 T. M. Li, G. W. Chen, C. C. Su, *et al.*, Ellagic acid induced p53/p21 expression, G1 arrest and apoptosis in human bladder cancer T24 cells, *Anticancer Res.*, 2005, **25**(2A), 971–980.
79 J. Dai and R. J. Mumper, Plant phenolics: extraction, analysis and their antioxidant and anticancer properties, *Molecules*, 2010, **15**(10), 7313–7352.
80 G. Galati and P. J. O'Brien, Potential toxicity of flavonoids and other dietary phenolics: significance for their chemopreventive and anticancer properties, *Free Radical Biol. Med.*, 2004, **37**(3), 287–303.
81 J. Madunic, I. V. Madunić, G. Gajski, J. Popic and V. Garaj-Vrhovac, Apigenin: a dietary flavonoid with diverse anticancer properties, *Cancer Lett.*, 2018, **413**, 11–22.
82 S. Khorrami, A. Zarrabi, M. Khaleghi, M. Danaei and M. Mozafari, Selective cytotoxicity of green synthesized silver nanoparticles against the MCF-7 tumor cell line and their enhanced antioxidant and antimicrobial properties, *Int. J. Nanomed.*, 2018, **13**, 8013–8024.

83 E. J. Park, J. Yi, Y. Kim, K. Choi and K. Park, Silver nanoparticles induce cytotoxicity by a Trojan-horse type mechanism, *Toxicol. In Vitro*, 2010, **24**(3), 872–878.
84 E. Bressan, L. Ferroni, C. Gardin, *et al.*, Silver nanoparticles and mitochondrial interaction, *Int. J. Dent.*, 2013, 1–8.
85 R. P. Singh and P. Ramarao, Cellular uptake, intracellular trafficking and cytotoxicity of silver nanoparticles, *Toxicol. Lett.*, 2012, **213**(2), 249–259.
86 V. Dhand, L. Soumya, S. Bharadwaj, S. Chakra, D. Bhatt and B. Sreedhar, Green synthesis of silver nanoparticles using Coffea arabica seed extract and its antibacterial activity, *Mater. Sci. Eng., C*, 2016, **58**, 36–43.
87 P. Palaniappan, G. Sathishkumar and R. Sankar, Fabrication of nano-silver particles using Cymodocea serrulata and its cytotoxicity effect against human lung cancer A549 cells line, *Spectrochim. Acta, Part A*, 2015, **138**, 885–890.
88 S. Thangapandiyan and P. Prema, Chemically fabricated silver nanoparticles enhances the activity of antibiotics against selected human bacterial pathogens, *Int. J. Pharm. Sci. Res.*, 2012, **3**(5), 1415–1422.
89 S. Rajeshkumar, C. Malarkodi, M. Vanaja and G. Annadurai, Anticancer and enhanced antimicrobial activity of biosynthesizd silver nanoparticles against clinical pathogens, *J. Mol. Struct.*, 2016, **1116**, 165–173.
90 A. Kedziora, W. Strek, L. Kepinski, G. Bugla-Ploskonska and W. Doroszkiewicz, Synthesis and antibacterial activity of novel titanium dioxide doped with silver, *J. Sol-Gel Sci. Technol.*, 2012, **62**(1), 79–86.
91 H. H. Bahjat, R. A. Ismail, G. M. Sulaiman and M. S. Jabir, Magnetic field-assisted laser ablation of titanium dioxide nanoparticles in water for anti-bacterial applications, *J. Inorg. Organomet. Polym. Mater.*, 2021, **120**, 1–8.
92 S. Rajeshkumar, J. Santhoshkumar, L. T. Jule and K. Ramaswamy, Phytosynthesis of Titanium Dioxide Nanoparticles Using King of Bitter Andrographis paniculata and Its Embryonic Toxicology Evaluation and Biomedical Potential, *Bioinorg. Chem. Appl.*, 2021, 1–11.
93 S. K. Chandraker, M. Lal, M. K. Ghosh, V. Tiwari, T. K. Ghorai and R. Shukla, Green synthesis of copper nanoparticles using leaf extract of Ageratum houstonianum Mill and study of their photocatalytic and antibacterial activities, *Nano Express*, 2020, **1**(1), 010033.
94 L. Chompunut, T. Wanaporn, W. Anupong, M. Narayanan, M. Alshiekheid, A. Sabour, I. Karuppusamy, N. T. L. Chi and R. Shanmuganathan, Synthesis of copper nanoparticles from the aqueous extract of Cynodon dactylon and evaluation of its antimicrobial and photocatalytic properties, *Food Chem. Toxicol.*, 2022, **166**, 113245.
95 K. Taghizadeh and Rad-Moghadam, Green fabrication of Cu/pistachio shell nanocomposite using Pistacia vera L. hull: an efficient catalyst for expedient reduction of 4-nitrophenol and organic dyes, *J. Cleaner Prod.*, 2018, **198**, 1105–1119.
96 M. A. Ahsan, V. Jabbari, A. A. El-Gendy, M. L. Curry and J. C. Noveron, Ultrafast catalytic reduction of environmental pollutants in water *via* MOF-derived magnetic Ni and Cu nanoparticles encapsulated in porous carbon, *Appl. Surf. Sci.*, 2019, **497**, 143608.
97 G. Wang., K. Zhao., C. Gao., J. Wang., Y. Mei., X. Zheng. and P. Zhu., Green synthesis of copper nanoparticles using green coffee bean and their applications for efficient reduction of organic dyes, *J. Environ. Chem. Eng.*, 2021, **9**(4), 105331.
98 A. Inoue, Y. Nishimura, N. Matsumoto, N. Umemoto, Y. Shimada, T. Maruyama, K. Kayasuga, M. Morihara, J. Katagi, T. Shiroya, *et al.*, Comparative study of the zebrafish embryonic toxicity test and mouse embryonic stem cell test to screen developmental toxicity of human pharmaceutical drugs, *Fundam. Toxicol. Sci.*, 2016, **3**, 79–87.
99 Z. Guan, S. Ying, P. C. Ofoegbu, P. Clubb, C. Rico, F. He and J. Hong, Green synthesis of nanoparticles: Current developments and limitations, *Environ. Technol. Innovation*, 2022, 102336.
100 S. A. Aromal and D. Philip, Facile one-pot synthesis of gold nanoparticles using tannic acid and its application in catalysis, *Phys. E*, 2012, **44**(7–8), 1692–1696.